$O(^1D) + N_2O$ Reaction: NO Vibrational and Rotational Distributions†

O. Tokel,‡ J. Chen, C. K. Ulrich,§ and P. L. Houston*

School of Chemistry and Biochemistry, Georgia Institute of Technology, Atlanta, Georgia 30332

Received: May 10, 2010; Revised Manuscript Received: August 12, 2010

The $O(^1D) + N_2O \rightarrow 2NO(X\ ^2\Pi)$ reaction has been studied in a molecular beam experiment in which O_3 and N_2O were coexpanded. The precursor $O(^1D)$ was prepared by O_3 photodissociation at 266 nm, and the $NO(X\ ^2\Pi)$ molecules born from the reaction as the $O(^1D)$ recoiled out of the beam were detected by 1+1 REMPI over the 220−246 nm probe laser wavelength range. The resulting spectrum was simulated to extract rotational and vibrational distributions of the $NO(X\ ^2\Pi)$ molecules. The product rotational distribution is found to be characterized by a constant rotational temperature of ≈4500 K for all observed bands, $v = 0-9$. An inverted vibrational distribution is observed. A consistent explanation of this and previous experimental results is possible if there are two channels for the reaction, one producing a nearly statistical vibrational distribution for low $O(^1D)-N_2O$ relative velocity collisions and a second producing the inverted distribution observed here for high relative velocity collisions. The former might correspond to an insertion/complex-formation reaction, while the latter might correspond to a stripping reaction. Velocity relaxation of the $O(^1D)$ is argued to compete strongly with reaction in most bulb studies, so that these studies see predominantly the nearly statistical distribution. In contrast, the beam experiments do not detect the part of the vibrational distribution produced in low relative velocity reactions because the $O(^1D)$ is not relaxed from its initial velocity before it either reacts or leaves the beam.

Introduction

The reaction between $O(^1D)$ and N_2O is of importance to atmospheric chemistry and is interesting from the point of view of a multichannel reaction:

$$O(^1D) + N_2O \rightarrow N_2 + O_2 \qquad k = 4.9 \times 10^{-11}\ cm^3\ molecule^{-1}\ s^{-1} \quad (1a)$$

$$\rightarrow NO + NO \qquad k = 6.7 \times 10^{-11}\ cm^3\ molecule^{-1}\ s^{-1} \quad (1b)$$

The reaction rate increases as the relative velocity between the $O(^1D)$ and N_2O decreases. The reaction is important to atmospheric chemistry because the branching ratio between the two channels is fundamental to the steady-state concentration of ozone.[1] N_2 and O_2 are major constituents of the stratosphere, so reaction to this channel is neutral to the concentration of ozone. Production of two NO molecules, however, decreases the ozone concentration because NO is a catalyst in a scheme that converts two ozone molecules to three molecules of oxygen. Thus, not only is the odd oxygen species $O(^1D)$ destroyed in (1b), but also the products go on to catalyze the destruction of further odd oxygen.

There is considerable uncertainty concerning the vibrational distribution of the NO products from reaction 1b; we summarize previous results briefly here and return to this issue in the discussion section. Brouard et al.[2,3] reported the stereochemistry of the reaction by probing NO in $v = 15$ and 16. Akagi et al.[4−6] reported that two different NO molecules were formed, a "new" one from the abstraction of an N atom by $O(^1D)$ from N_2O and the other from the "old" NO left behind. By using isotopic labeling, they found that the new NO had a peak in the vibrational distribution at high vibrational levels, whereas the old one peaked at $v = 0$. Pisano et al. reported the distribution from $v = 0$ to $v = 12$ and found it to peak at $v = 7$.[7] Hancock and Haverd measured time-resolved infrared emission of NO(v = 1−14) and concluded that the vibrational distribution for these states decreased monotonically from a maximum population at $v = 1$.[8] An earlier paper using this technique was reported by Wang et al.[9] Finally, Lu, Liang, and Lin have recently investigated the translational energy distribution of the $N_2 + O_2$ and NO + NO products from the $O(^1D) + N_2O$ reaction.[10] For the NO + NO products, they report that the translational energy release consumes 31% of the available energy. It remains unclear from these studies both what the vibrational distribution actually is and why so many measurements differ from one another. All attempts to measure the nascent rotational distribution find that it is very hot. Kawai et al.[11] report temperatures up to 20 000 K, while Tsurumaki et al.[12] found 10 000 K.

The reaction of $O(^1D)$ with N_2O has also been investigated in clusters, typically by photodissociation of one N_2O of the N_2O dimer.[13,14] This "pre-aligned" reaction produces NO vibrational excitation, but it may be somewhat different from that of the normal reaction. In particular, it appears that the rotational temperatures of the NO products are typically colder, on the order of 60−100 K, than those reported for the normal reaction described above.

Theoretical investigations of the $O(^1D) + N_2O$ reaction are limited. Gonzalez and co-workers performed trajectory calculations using both A′ and A″ surfaces calculated at the CASPT2/CASSCF level.[15−17] Last et al. have investigated the $O(^1D) + N_2O$ reaction on an ab initio surface calculated using the Møller−Plesset method.[18] More recently, Akagi et al.[19] devel-

† Part of the "Klaus Müller-Dethlefs Festschrift".

* To whom correspondence should be addressed.

‡ Also School of Applied and Engineering Physics, Cornell University, Ithaca, NY 14853.

§ Also Department of Chemistry, Cornell University, Ithaca, NY 14853.

10.1021/jp1042377
Published on Web 08/24/2010

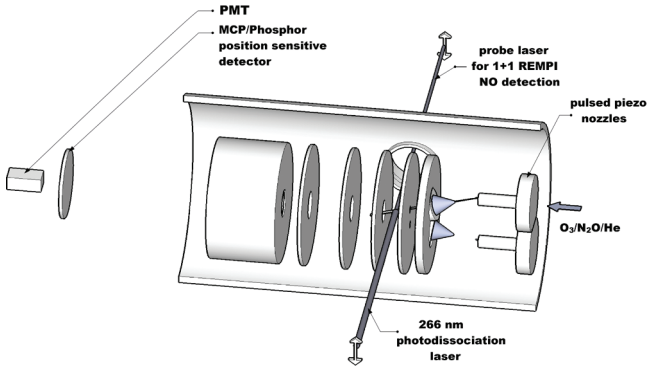

Figure 1. Scaled diagram of the experimental apparatus.

oped a surface at the CASPT2/cc-pVDZ level for the reaction, and Takayanagi and Akagi have reported the results of classical trajectory studies.[20] Finally, Takayanagi has performed mixed quantum-classical wavepacket calculations to explore this system.[21]

In this paper we report a detailed investigation of the vibrational and rotational distribution of the NO product of (1b) using multiphoton ionization to probe the NO product following reaction of O(^{1}D) and N_2O in a molecular beam.

Experimental Section

Figure 1 presents a schematic drawing of the experimental apparatus. The molecular beam setup is a modified version of the single beam ion imaging apparatus described elsewhere.[7] In a manner similar to the setup first described by Welge and co-workers,[22] a second nozzle has been added parallel to the first one in preparation for future reaction product imaging studies. The apparatus has been equipped with additional electrodes for dc or pulsed slice imaging capabilities when desired.

A mixture of O_3 (1%) and N_2O (6%) seeded in He (backing pressure 2 psi) was expanded supersonically through a 500 μm diameter nozzle, and collimated with a 500 μm diameter skimmer located 2 cm from the nozzle. Two unfocused counterpropagating laser beams intersected the molecular beam at right angles in the center of the repeller and extractor electrodes and 7.5 cm from the nozzle. One laser dissociated the O_3 molecules to generate O(^{1}D) atoms, while the other state selectively ionized the resulting NO($X^2\Pi$) molecules formed in the O(^{1}D) + $N_2O \rightarrow 2NO(X\ ^2\Pi)$ reaction. The ion cloud was then extracted through an optimized velocity-map spectrometer and impinged onto a gated dual microchannel plate coupled to a fast phosphor screen (Burle, P-47) located at the end of the time-of-flight tube. The ion intensity was measured with a PMT (Thorn EMI) and passed to a computer, where a boxcar records the NO signal strength as a function of laser wavelength.

The O_3 molecules were dissociated by the linearly polarized 266 nm laser light generated by the fourth harmonic of a Nd:YAG laser (Spectra-Physics GCR-6) operating at 10 Hz. Typical energies were 5−6 mJ/pulse. The laser beam size was apertured to 5 mm, which gave the maximum signal-to-noise ratio under our detection conditions. The polarization axis of the dissociation light was vertical to the plane defined by the molecular beam and the 266 laser direction.

The O(^{1}D) ions created by a 203.7 nm, 2+1 REMPI processes,[23] were used to check the molecular beam properties and to optimize production of this species. The 203.7 nm light was generated by doubling the output of a Nd:YAG (Spectra-Physics GCR-270) pumped dye laser (PDL-2) in a KDP crystal and then summing the fundamental with the doubled light in a BBO crystal. Typical powers were 0.9 mJ/pulse at 10 Hz.

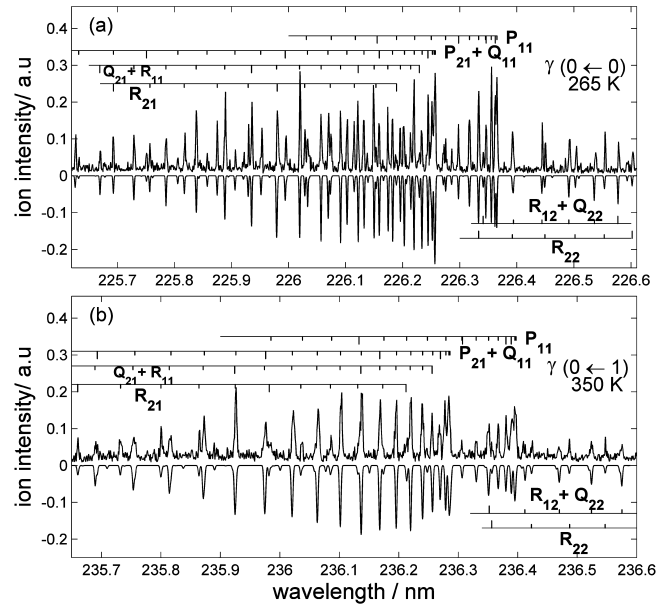

Figure 2. NO^+ ion signal from (a) probe laser, $v = 0$, and (b) probe + N_2O, $v = 1$. The upper plot shows the data and the lower one is the simulated spectrum.

NO molecules were state-selectively detected by a 1+1 REMPI processes.[24,25] The tunable 220−246 nm laser light used to probe the NO molecule was generated by doubling the output of a Nd:YAG (GCR-230) pumped Scanmate OPPO laser (Lambda Physik). The probe laser polarization was the same as that of the 266 nm laser. The probe laser was set to arrive 20 ns after the 266 nm laser. To generate the appropriate light, three types of dye were used: Coumarin 450, 460, and 480. Typical energies were 0.9−1 or 0.5−0.6 mJ/pulse. The pulse energy levels were chosen so that the NO ion signal did not saturate. Care was also taken by routinely monitoring the signal under small magnetic fields to ensure that no electrons generated by secondary processes caused any ion background. A series of overlapping 1.5 nm scans were recorded at 30 laser shots/step, monitoring the laser pulse energies before and after each scan.

Ultrahigh purity N_2O (99.99%) and He (99.999%) were purchased from Matheson Tri-Gas and Airgas, respectively, and used without any further purification. O_3 was generated by a commercial ozonator and kept in a silica gel trap at −78 °C.[26]

Results

Background Sources. There are three possible NO background sources in the experiment. First, some residual NO molecules are in thermal contact with the chamber walls. At 300 K these molecules account for almost all the thermal NO molecules populating $v = 0$ and around 0. 01% of those populating the $v = 1$ level. This source was very small compared to our signal, 3−4% for $v = 0$. The signal for NO($X\ ^2\Pi$) ($v = 0$) from this source has been characterized, as shown in Figure 2a, which is a scan of the probe laser with the molecular beam off.

A second background source is the NO generated and detected by the interaction of N_2O and the probe laser; that is, the background is there even when there is no ozone in the beam mixture and when the 266 nm light is blocked. The background

was weak; we estimate it to account for less than 7% of the signal in $v = 0$. To characterize this background source for higher vibrational levels, we put pure N_2O in the beam and scanned the probe laser wavelength over strong transitions used for NO($X\ ^2\Pi$) $v = 1$, 2, and 3 detection. Figure 2b shows the N_2O + probe laser scan for NO($X^2\Pi$) ($v = 1$). Similar but much weaker beam-dependent spectra have been obtained for NO($X^2\Pi$) $v = 2$ and 3, with rotational temperatures close to 300 K, but the signal was too weak for a proper fit.

Honma and co-workers have shown that N_2O dimers formed in the molecular beam can be photolyzed by 193 nm photons, creating NO($X^2\Pi$) through the $O(^1D)\cdot N_2O$ reactant pair.[13] Gödecke et al.[14] have recently studied the same reaction. They report rotational temperatures around 150 K, whereas Honma and co-workers report 60−100 K for all vibrational levels up to $v = 7$. Our $v = 1$ scan showed a rotational temperature around 350 K, much higher than that found from the dimer experiments. Thus, it seems unlikely that dimers are the source of this background.

Whatever the source of the background, in our experiments performed with the O_3/N_2O mixture, the $v = 0$ background contribution from this beam dependent source is less than 7% of our net signal, and higher levels are absent. Apart from their small intensity in the experiment, both the first and second background sources have a T_{rot} around 300 K, much lower in comparison to that found for vibrational levels monitored in the full experiment on the O_3/N_2O mixture. In summary, the second background makes a small contribution, but only to $v = 0$.

The total background in the scans is around 10−15%, and much of this belongs to a third source of NO. Analysis of this source shows that it is a scaled down version of our actual experimental signal. This can be understood as a result of dissociation of O_3 by the probe laser.

Dissociation of ozone is through the Hartley band, which peaks at 254 nm. Absorption of a photon in this band results mostly in photodissociation through two channels, both of which create translationally hot $O(^1D)$ atoms.[27,28] The $O_3 + h\nu \rightarrow O_2(a\ ^1\Delta_g) + O(^1D)$ channel opens for $\lambda < 310$ nm, whereas the $O_3 + h\nu \rightarrow O_2(b\ ^1\Sigma^+_g) + O(^1D)$ channel opens for $\lambda < 267$ nm. About 90% of the dissociation in this band proceeds by the first channel. Since our probe laser scans extend to the middle of the Hartley band, it is to be expected that some O_3 molecules will dissociate by this channel after absorbing the probe laser light. The resulting $O(^1D)$ atoms would react with the N_2O, creating NO molecules, which are then ionized by the same pulse. Fortunately, this is a multiphoton process, so the signal is not too large with our unfocused laser pulses. Furthermore, the O_3 absorption cross section at the wavelengths used for probing NO is small compared to that at 266 nm, and the probe pulse energy is a factor of 5 smaller than that of the 266 pulse. All of these factors result in a small magnitude for the background signal caused by the probe laser. That this background closely mimics the actual signal is not surprising, considering that the difference between the relative collision energies of the precursor $O(^1D)$ atoms created by two lasers is much smaller than the large exothermicity of the reaction.[15,27]

Analysis Procedure. A preliminary analysis of the 1+1 REMPI spectrum was required due to the very hot rotational temperature observed. Pisano et al. have shown that the rotationally cooled spectrum is dominated by γ transitions.[7] A cross-correlation algorithm was written for calibrating the spectrum with γ transitions only, simulated with LIFBASE[29] software, assuming an initial rotational and vibrational temperature.

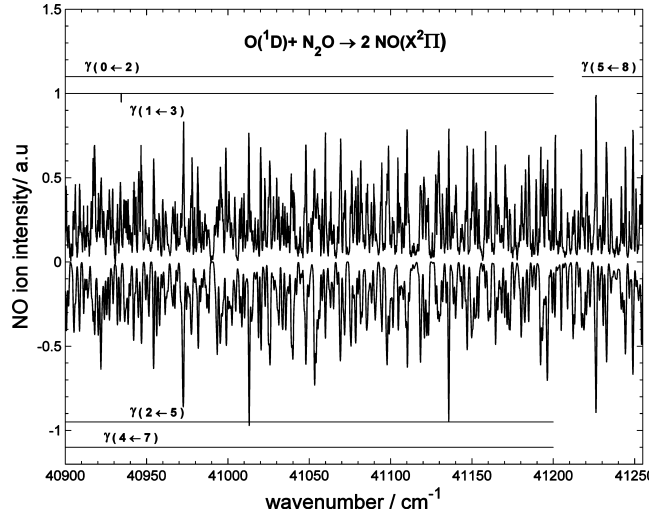

Figure 3. 1+1 REMPI spectrum of NO($X\ ^2\Pi$) from the $O(^1D)$ + $N_2O \rightarrow 2NO(X\ ^2\Pi)$ reaction. Features from the A ← X (0,2); (1,3); (2,5); and (4,7) bands span the whole range. The (5,8) band head and (1,3) band origin are also shown. The upper plot shows the data and the lower one is the simulation with $T_{rot} = 4500$ K.

To determine the relative population of each NO($X\ ^2\Pi$) vibrational level produced in the reaction, we modeled the NO γ and β transitions with Pgopher.[30] Fermi's golden rule states that the one photon transition probability is proportional to the square of the $\langle \mu \cdot E \rangle$ matrix element, where E is the polarization vector of our linearly polarized probe laser and μ is the molecule's transition dipole moment. Therefore, we need to use only first-order spherical transition moments in the simulation, i.e., electric dipole moments. The spectroscopic constants for the ground state NO($X\ ^2\Pi$) are taken from Amiot[31] and Engelman et al.,[32,33] and for the NO($B^2\Pi$) state from Huber and Herzberg[34] and Hamilton et al.[35] The NO($A\ ^2\Sigma$) state has been recently revisited by Danielak and co-workers.[36] Since the observed spectrum is rotationally hot, the rotational constants B_v and D_v are statistically significant. For the β system, the D_v values are less certain, so we used the set of rotational constants from Hamilton et al., derived from the literature in a self-consistent manner.

The following procedure was followed for the analysis. First, a constant rotational temperature, T_{rot}, is assumed for all vibrational levels. A section of the data is picked and an iterative fitting is performed for all individual γ bands extending into the chosen region. Because the γ and β bands are two competing absorption systems with different ionization efficiencies, one needs to also check for β bands in each region.[37] Thus, the same iteration is repeated for β transitions in each data segment. After an initial fit, the iteration moves to a neighboring section. Once a reasonable fit is obtained to all the data segments, the iteration set is repeated over the whole of the spectrum again, but this time including the T_{rot} as a fitting parameter in the set. The iterations are continued until satisfactory convergence is attained to the data.

The second step is to relax the universal temperature constraint for the main bands contributing to the data; a band by band individual T_{rot} fit is performed, allowing for differences in T_{rot} with vibrational level. A Boltzmann rotational distribution is assumed in all fits.

Discussion

Vibrational Distribution. A portion of the recorded spectrum[38] is shown in Figure 3, along with the best fit that resulted

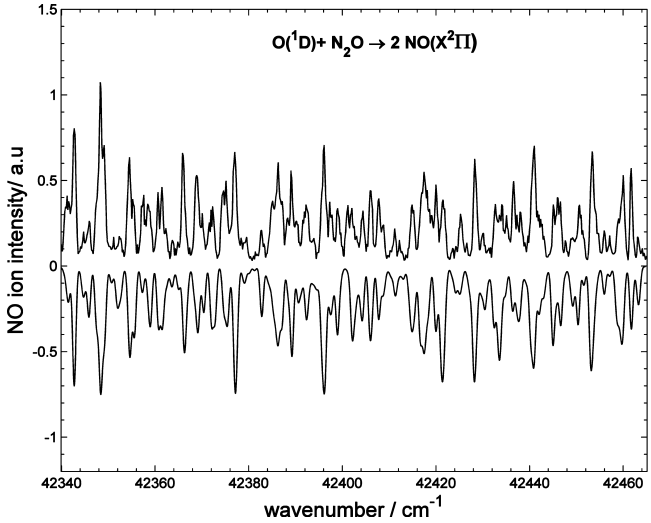

Figure 4. 1+1 REMPI spectrum of NO(X $^2\Pi$) from the $O(^1D) + N_2O \rightarrow 2NO(X\ ^2\Pi)$ showing a smaller spectral region expanded so as to demonstrate the degree of agreement between the measured spectrum (upper plot) and the calculated one (lower plot). The $\gamma(0,1)$ and $\gamma(3,5)$ transitions span the entire area with contributions from the $\gamma(4,6)$ transitions.

from the procedure described above. Figure 4 shows an expanded version in more detail. The individual T_{rot} fits showed that the observed vibrational transitions can be well represented by a Boltzmann rotational distribution with a universal T_{rot} around 4500−5000 K. Tsurumaki et al.[12] have measured the rotational temperature of NO($v = 0$) with Doppler-resolved LIF, via the $\gamma(0,0)$ band for the same reaction, using 193 nm laser pulses to generate the $O(^1D)$ precursor from N_2O. Their reported T_{rot} of 10 000 K contrasts with the 300 K reported by Brouard et al.[2] for the same system. However, both observed very high rotational temperatures for $v > 0$, with Brouard et al. reporting $T_{rot} = 5500$ K, for $v = 1$. The discrepancy at $v = 0$ was probably because of the thermal NO ($v = 0$) in the chamber, dominating the LIF signal in the latter experiment. Kawai et al.[11] recently determined the rotational temperature as ≈20 000 K for NO ($v = 0, 1, 2$) for the part of the distribution with $J < 80$, as measured under flow conditions. For $J > 80$, they observe a faster decrease in their distribution, corresponding to a somewhat lower rotational temperature. In our fits to the data, we did not observe strong differences from a Boltzmann distribution for $J > 80$ populations.

The contributing transitions in the 220−246 nm range were found to be only the γ transitions. Akagi[4,6] have used the B $^2\Pi(v = 0-2) \leftarrow$ X $^2\Pi(v = 11-17)$ transitions for the LIF detection, and Pisano et al.[7] observed the NO β system REMPI for this reaction, but both had rotationally cooled sources, allowing them to isolate these tiny signals from the otherwise congested spectrum. The NO molecule is very efficiently detected with REMPI processes,[37] so under cooled conditions the β system would be an additional source of information.

The electric dipole transition matrix element fit parameter input to the Pgopher program can be converted to relative vibrational populations for each band, using the known electronic transition moments, $R_e(r_{v',v''})$[39] and Franck−Condon factors.[39,40] The relative vibrational populations are given in Table 1.

Origin of Vibrational Excitation. The origin of the inverted vibrational distributions can be qualitatively understood by considering the two competing factors affecting it, the energy randomization rate in the intermediate and the available time for this randomization to take place. Ab initio calculations of potential energy surfaces[16,17,43] show that the NO + NO products correlate on two 1A″ surfaces and one 1A′ surface to $O(^1D) + N_2O$. All surfaces for $O(^1D) + N_2O$ leading to NO + NO products pass through a dimer configuration. The lifetime of the intermediate for this reaction is estimated to be on the order of 1 ps or less,[12,44] on the order of the rotational period of the *cis*-NO dimer.[12] Considering the large exothermicity and the barrierless PES for the reaction, with this seemingly short-lived intermediate, the NO can be expected to show characteristics of a nonstatistical vibrational distribution, rather like the inverted vibrational distribution for the new OH product in the $O(^1D) + H_2O$[45,46] reaction, as compared to the old OH from the original water, which shows a colder vibrational distribution in comparison to a statistical one. However, in the reaction we are studying, this effect is counterbalanced by intramolecular vibrational relaxation (IVR), which is proportional to the density of states in the intermediate and to the square of the effective coupling between the vibrational states. The two similar masses of the NO molecules are likely to increase the density of states available in the intermediate, as discussed by Akagi et al.[5] Kawai et al. confirm that the stretching modes are strongly coupled for the reaction path which passes through the trans-minimum.[43] These two competing mechanisms are likely to end up leaving NO molecules with an inverted vibrational distribution under high energy collisions with a direct mechanism, and possibly with more chance of energy redistribution at lower energy collisions.

TABLE 1: NO(X$^2\Pi$) Vibrational-State Distribution of $O(^1D) + N_2O \rightarrow 2NO(X\ ^2\Pi)$

vibrational state	observed transition(s)	relative populations[a]	weighted average[b]
0	$\gamma(0,0)$	0.088 ± 0.008	0.089 ± 0.008
1	$\gamma(0,1)$	0.036 ± 0.003	0.039 ± 0.010
	$\gamma(1,1)$	0.075 ± 0.014	
2	$\gamma(0,2)$	0.041 ± 0.004	0.043 ± 0.003
	$\gamma(2,2)$	0.047 ± 0.009	
3	$\gamma(1,3)$	0.125 ± 0.010	0.116 ± 0.015
	$\gamma(2,3)$	0.095 ± 0.014	
4	$\gamma(3,4)$	0.098 ± 0.015	0.100 ± 0.015
5	$\gamma(4,5)$	0.134 ± 0.021	0.212 ± 0.026
	$\gamma(3,5)$	0.220 ± 0.011	
	$\gamma(2,5)$	0.242 ± 0.019	
6	$\gamma(4,6)$	0.128 ± 0.014	0.130 ± 0.015
7	$\gamma(6,7)$	0.095 ± 0.026	0.124 ± 0.024
	$\gamma(5,7)$	0.103 ± 0.016	
	$\gamma(4,7)$	0.173 ± 0.021	
8	$\gamma(6,8)$	0.118 ± 0.025	0.093 ± 0.015
	$\gamma(5,8)$	0.084 ± 0.014	
9	$\gamma(6,9)$	0.053 ± 0.015	0.054 ± 0.015

[a] The relative vibrational distribution from each band is given before averaging and weighing the data. Since the fluctuations of error in the bands occurring in the same spectral region are correlated, about a ±15% fit precision to peak height is assumed in the error calculations. The uncertainties include the estimated uncertainty in the transition probabilities. Transition probabilities for bands $\gamma(6,7)$, $\gamma(6,8)$, and $\gamma(6,9)$ were taken from ref 40 and carry higher uncertainties because a Morse oscillator wave function is assumed. [b] The weighted mean and error in the weighted mean are calculated using eqs 4.21 and 4.22 from ref 41. Following averaging, the weighted mean is normalized to a sum of unity over all observed levels.

Importance of $O(^1D)$ Velocity Relaxation. An important question to address is why there is so much discrepancy between the various measurements of the NO vibrational distribution produced following reaction of $O(^1D)$ with N_2O. Hancock and Haverd provided a very thoughtful discussion of the potential

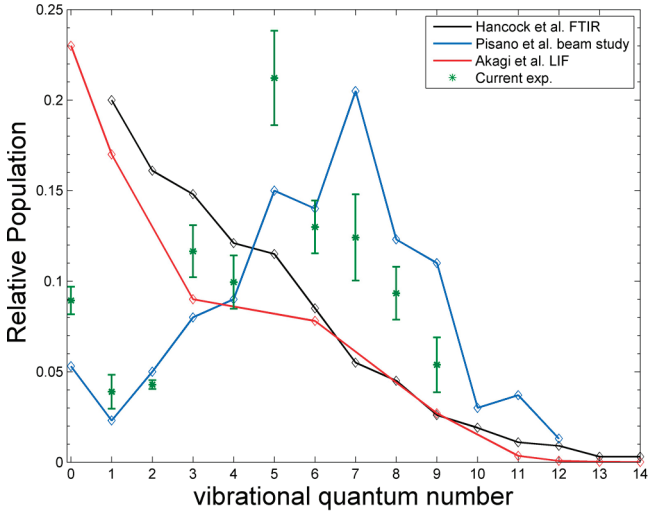

Figure 5. Comparison of the relative NO(X $^2\Pi$) vibrational level population results from the current experiment with those from previous molecular beam and bulk studies. A shoulder is observed in the $v = 4-8$ range in the bulk studies, whereas an inverted population is observed in the molecular beam studies.

problems in each of the reported experiments, but they were still at a loss to explain the discrepancies shown in their Figure 4.[8] These distributions, along with results from the current study (plotted as weighted averages from Table 1), are shown in Figure 5. An alternate approach is to ask if there might be some hidden variable that has hitherto been unaccounted for; perhaps all the measurements are correct, but there is a difference in conditions that has not been noticed. We argue here that the hidden variable is the velocity distribution associated with the collision between $O(^1D)$ and N_2O.

The experiments are of two broad types. The first type are those done in a molecular beam, including that by Pisano et al.,[7] that by Lu, Liang, and Lin,[10] and the current experiment. The second type are those done in static or flowing bulb experiments. The conditions for the latter are as follows. Akagi et al. generated $O(^1D)$ from 266 nm photolysis of O_3 and performed the experiment at a total pressure of 1.0 Torr at a delay time of 5 μs.[4,6] Brouard et al. used 193 nm photodissociation of N_2O as an $O(^1D)$ source and performed the experiment at a total pressure of up to 200 mTorr with a delay time of 200 ns.[2,3] Hancock and Haverd used a similar source with a total pressures of 0.3−1.0 Torr and a delay time of around 40 μs.[8]

The conditions for the molecular beam experiments are as follows. Pisano et al.[7] used a molecular beam experiment in which an O_3/N_2O mixture was photolyzed at 266 nm near the throat of a nozzle expansion. Most $O(^1D)$ atoms flew out of the beam before reacting, but those that reacted did so within roughly a single collision. The resulting NO was rotationally relaxed by collisions in the expansion, but vibrational relaxation under such conditions is negligible. The NO products were detected downstream, in the collisionless part of the beam, by a 1+1′ REMPI scheme. Because of the rotational relaxation, the spectra were simpler to interpret than those in the current experiment. The conditions for the current experiment are similar to those used by Pisano et al. in that a molecular beam of an O_3/N_2O mixture is employed with photodissociation at 266 nm, but both dissociation and detection are accomplished in the collisionless part of the beam. Again, most of the $O(^1D)$ products escape from the beam, but a few collide with N_2O to produce NO products, which are probed withing a delay time of 20 ns. These products presumably have the vibrational and rotational distributions characteristic of a single collision at high velocity. The velocity distribution of the $O(^1D)$ in the current and Pisano et al. experiments is peaked at 2.2×10^5 cm/s. Lu, Liang, and Lin used a crossed molecular beam apparatus.[10] The $O(^1D)$ was produced by 157 nm photolysis of O_2, giving a velocity of 2.1×10^5 cm/s.

While much attention in the bulb experiments has been focused on the possibility of vibrational relaxation of the NO, the possibility of velocity relaxation of the $O(^1D)$ has not been considered. We hypothesize that "slow" $O(^1D)$ reacts with N_2O to give a statistical vibrational distribution, perhaps through an insertion/complex-forming process, whereas "fast" $O(^1D)$ reacts to give an inverted distribution, through a more direct mechanism. For any individual experiment, the result would then be a weighted sum of the statistical distribution, given by the data of Akagi et al.[6] in our Figure 5, and an inverted distribution given by the current data, also shown in our Figure 5. The distributions of Akagi et al. (Figure 3),[6] and of Hancock and Haverd (Figure 5)[8] do seem to show a shoulder at $v = 4-8$ on top of a more statistical distribution, albeit one that peaks at the lowest vibrational level. Thus, our hypothesis is that the $O(^1D)$ reacts from a relaxed velocity distribution in the bulb experiments, favoring the statistical branch of the NO vibrational distribution. In the beam experiments, on the other hand, if the $O(^1D)$ produced by the reaction does not react on its first collision with N_2O, it leaves the beam and does not react at all. Thus, it reacts with the velocity provided by the O_3 dissociation, a velocity high enough to favor the stripping branch of the NO vibrational distribution.

The only potential counterexample to this interpretation is the result by Lu, Liang, and Lin.[10] Although they do not directly measure the NO vibrational or rotational distribution, they find that the translational energy deposition in the reaction is 31% (28 kcal/mol out of 89.7 kcal/mol available), a value too high in their view to allow for the high vibrational and rotational excitation observed in the current experiments and in those of Pisano et al. Our own measurement of the rotational temperature suggests that the total rotational energy for the two fragments is less than 20 kcal/mol (out of 91.5 kcal/mol available). That would still leave roughly 42 kcal/mol available for vibration, or about 47%. While this fraction is less than the 75−87% estimate of Pisano et al., it still means that the average NO molecule would have 21 kcal/mol in vibration and would be at $v = 4$, as compared to the peak of the distribution at $v = 5$ in the current experiment. To be completely consistent with our measurement, the translational energy disposal would need to be only 18 kcal/mol, as compared with their measurement of 28 kcal/mol.

Some estimates show the plausible importance of velocity relaxation. The total rate constant for reaction of $O(^1D)$ with N_2O is 1.2×10^{-10} cm^3 molecule^{-1} s^{-1}. Measurements have been made on the relaxation of $S(^1D)$ velocities in collisions with He, Ar, and Xe[47] and of $O(^1D)$ velocities in collisions with He, Ne, Ar, N_2, and O_2.[48,49] For $O(^1D)$ with N_2, the rate of velocity relaxation is 1.99×10^{-10} cm^3 molecule^{-1} s^{-1}. Assuming the velocity relaxation cross section for $O(^1D) + N_2O$ to be similar to that for $O(^1D) + N_2$, velocity relaxation is 1.7 times faster than the total reaction rate. Thus, the $O(^1D)$ in bulb experiments is cooling translationally nearly twice as fast as it is reacting. While the $O(^1D) + N_2O$ relaxation rate might be somewhat dissimilar from that for $O(^1D) + N_2$, the fact that the rates of velocity relaxation of $O(^1D)$ and $S(^1D)$ by nearly all measured partners are comparable suggests that the conclusion that velocity relaxation competes effectively with reaction

is likely to be a robust one. Repetition of previous experiments but with N_2O as the target could confirm this conclusion. However, given the current state of knowledge it appears plausible that under the bulb conditions, the reaction might favor predominantly a statistical distribution whereas under beam conditions it might favor predominantly an inverted distribution.

A molecular beam experiment might be designed to check this hypothesis by using slower $O(^1D)$ atoms to initiate the reaction. In such an experiment in the current apparatus, ozone would need to be dissociated with wavelengths longer than 290 nm for the reaction to have small collision energies comparable to those in a cell experiment. Unfortunately, the ozone dissociation cross section is about an order of magnitude smaller at these wavelengths. Our estimate is that the ratio of signal to "probe laser and beam background" would be only around 1. Furthermore, the probe laser would still create fast $O(^1D)$ atoms that would complicate the interpretation. Thus, this experiment was not attempted.

Conclusions

An inverted vibrational and a very hot rotational distribution is observed in the NO product channel of N_2O collisions with fast $O(^1D)$ atoms. The translational relaxation of $O(^1D)$ in bulb experiments probing the same reaction is hypothesized to play a role in their observation of colder and more statistical NO vibrational distributions.

We conclude that an inverted vibrational distribution in this channel is likely be the result of a direct reaction mechanism, whereas a statistical outcome can dominate at lower collison energies through an insertion type mechanism and with the help of efficient coupling of NO stretching modes in the collision complex.

Extending the reduced dimensionality QCT calculations[42,44] to full three dimensions may shed light on the origins of the observed distribution. Experimentally, isotopically labeled species can be used to get more information on this channel, if a 2-fold congested spectrum can be similarly analyzed. A more informative study would be a state-selected crossed molecular beam investigation, which is currently underway in our lab. In this experiment, ozone is dissociated in one beam, and the product $O(^1D)$ flies to a beam of N_2O, where reaction takes place. Separating the location of the probe laser from the ozone source circumvents creation of fast $O(^1D)$ by the probe laser, but the signal is still expected to be small due to the necessity of creation of slow $O(^1D)$ at wavelengths where ozone does not absorb strongly.

Acknowledgment. We gratefully acknowledge support for this work from the National Science Foundation under award CHE-0852482.

Supporting Information Available: Figure of the 1+1 REMPI spectrum of $NO(X^2\Pi)$ produced in the $O(^1D) + N_2O$ reaction spanning the range from about 40 800−43 300 cm^{-1}. This material is available free of charge via the Internet at http://pubs.acs.org.

References and Notes

(1) Wiesenfeld, J. R. *Acc. Chem. Res.* **1982**, *15*, 110–116.
(2) Brouard, M.; Duxon, S. P.; Enriquez, P. A.; Sayos, R.; Simons, J. P. *J. Phys. Chem.* **1991**, *95*, 8169–8174.
(3) Brouard, M.; Duxon, S. P.; Enriquez, P. A.; Simons, J. P. *J. Chem. Phys.* **1992**, *97*, 7414–7422.
(4) Akagi, H.; Fujimura, Y.; Kajimoto, O. *J. Chem. Soc., Faraday Trans.* **1998**, *94*, 1575–1581.
(5) Akagi, H.; Fujimura, Y.; Kajimoto, O. *J. Chem. Phys.* **1999**, *110*, 7264–7272.
(6) Akagi, H.; Fujimura, Y.; Kajimoto, O. *J. Chem. Phys.* **1999**, *111*, 115–122.
(7) Pisano, P. J.; Westley, M. S.; Houston, P. L. *Chem. Phys. Lett.* **2000**, *318*, 385–392.
(8) Hancock, G.; Haverd, V. *Phys. Chem. Chem. Phys.* **2003**, *5*, 2369–2375.
(9) Wang, X. B.; Li, H. Z.; Zhu, Q. H.; Kong, F. N.; Yu, H. G. *J. Chin. Chem. Soc.* **1995**, *42*, 399–403.
(10) Lu, Y.-J.; Liang, C.-W.; Lin, J. J. *J. Chem. Phys.* **2006**, *125*, 133121.
(11) Kawai, S.; Fujimura, Y.; Kajimoto, O.; Takayanagi, T. *J. Chem. Phys.* **2004**, *120*, 6430–6438.
(12) Tsurumaki, H.; Fujimura, Y.; Kajimoto, O. *J. Chem. Phys.* **1999**, *111*, 592–599.
(13) Honma, K.; Fujimura, Y.; Kajimoto, O.; Inoue, G. *J. Chem. Phys.* **1988**, *88*, 4739–4747.
(14) Gödecke, N.; Maul, C.; Chichinin, A. I.; Kauczok, S.; Gericke, K. H. *J. Chem. Phys.* **2009**, *131*, 054307-1−054307-11.
(15) Gónzales, M.; Troya, D.; Puyuelo, M. P.; Sayós, R.; Enrνquez, P. A. *Chem. Phys. Lett.* **1999**, *300*, 603–612.
(16) Gónzales, M.; Valero, R.; Anglada, J. M.; Sayós, R. *J. Chem. Phys.* **2001**, *115*, 7015–7031.
(17) Gónzales, M.; Sayós, R.; Valero, R. *Chem. Phys. Lett.* **2002**, *355*, 123–132.
(18) Last, I.; Aguilar, A.; Sayos, R.; Gonzalez, M.; Gilibert, M. *J. Phys. Chem. A* **1997**, *101*, 1206–1215.
(19) Akagi, H.; Yokoyama, A.; Fujimura, Y.; Takayanagi, T. *Chem. Phys. Lett.* **2000**, *324*, 423–429.
(20) Takayanagi, T.; Akagi, H. *Chem. Phys. Lett.* **2002**, *363*, 298–306.
(21) Takayanagi, T. *Chem. Phys.* **2005**, *308*, 211–216.
(22) Schnieder, L.; Seekamp-Rahn, K.; Liedeker, F.; Steuwe, H.; Welge, K. H. *Faraday Discuss. Chem. Soc.* **1991**, *91*, 259–269.
(23) Pratt, S. T.; Dehmer, P. M.; Dehmer, J. L. *Phys. Rev. A.* **1991**, *43*, 4702–4711.
(24) Hippler, M.; Pfab, J. *Chem. Phys. Lett.* **1995**, *243*, 500–505.
(25) Uberna, R.; Hinchliffe, R. D.; Cline, J. *J. Chem. Phys.* **1996**, *105*, 9847–9858.
(26) Stevens, R. E.; Hsiao, C. W.; Curro, L. L. N. J.; Monton, B. J.; Chang, B. Y.; Kung, C. Y.; Kittrell, C.; Kinsey, J. L. *Rev. Sci. Instrum.* **1998**, *69*, 2504–2508.
(27) Dylewski, S. M.; Geiser, J. D.; Houston, P. L. *J. Chem. Phys.* **2001**, *115*, 7460–7473.
(28) Takahashi, K.; Taniguchi, N.; Matsumi, Y.; Kawasaki, M. *Chem. Phys.* **1998**, *231*, 171–182.
(29) Luque, J.; Crowley, D. *LIFBASE: Database and spectral simulation*, version 1.5; 1999.
(30) Western, C. Pgopher, a Program for Simulating Rotational Structure, http://pgopher.chm.bris.ac.uk/.
(31) Amiot, C. *J. Mol. Spectrosc.* **1982**, *94*, 150–172.
(32) Engelman, R.; Rouse, P. E.; Peek, H. M.; Baiamonte, V. D. *The Beta and Gamma Systems of Nitric Oxide*; Los Alamos Scientific Report LA-4364; Los Alamos National Laboratory: Los Alamos, NM, 1970.
(33) Engelman, R.; Rouse, P. E. *J. Mol. Spectrosc.* **1971**, *37*, 240–251.
(34) Huber, K. P.; Herzberg, G.; Nostrand, V. *Molecular Spectra and Molecular Structure: IV. Constants of Diatomic Molecules*; 1970.
(35) Hamilton, P. A.; Phillips, A. J.; Windsor, R. *Chem. Phys. Lett.* **1997**, *264*, 245–251.
(36) Danielak, J.; Domin, U.; Kepa, R.; Rytel, M.; Zachwieja, M. *J. Mol. Spectrosc.* **1997**, *181*, 394–402.
(37) Jacobs, D. C.; Zare, R. N. *J. Chem. Phys.* **1986**, *85*, 5457–5468.
(38) Tokel, O. Ph.D. Thesis, 2010, to be published.
(39) Luque, J.; Crosley, D. R. *J. Chem. Phys.* **1999**, *111*, 7405–7415.
(40) Ory, H. A.; Gittleman, A. P.; Maddox, J. P. *Astrophys. J.* **1964**, *139*, 346–356.
(41) Bevington, P. R.; Robinson, D. K. *Data Reduction and Error Analysis for the Physical Sciences*.
(42) Takayanagi, T.; Wada, A. *Chem. Phys.* **2001**, *269*, 37–47.
(43) Kawai, S.; Fujimura, Y.; Kajimoto, O.; Yamashita, T.; Li, C. B.; Komatsuzaki, T.; Toda, M. *Phys. Rev. A* **2007**, *75*, 022714-1−022714-11.
(44) Kawai, S.; Fujimura, Y.; Kajimoto, O.; Yamashita, T. *J. Chem. Phys.* **2006**, *124*, 184315−1–184315−9.
(45) Cleveland, C. B.; Wiesenfeld, J. R. *J. Chem. Phys.* **1992**, *96*, 248–255.
(46) Sauder, D. G.; Stephenson, J. C.; King, D. S.; Casassa, M. P. *J. Chem. Phys.* **1992**, *97*, 952–961.
(47) Nan, G.; Houston, P. L. *J. Chem. Phys.* **1992**, *97*, 7865–7872.
(48) Matsumi, Y.; Shamsuddin, S. M.; Sato, Y.; Kawasaki, M. *J. Chem. Phys.* **1994**, *101*, 9610–9618.
(49) Taniguchi, N.; Hirai, K.; Takahashi, K.; Matsumi, Y. *J. Phys. Chem. A* **2000**, *104*, 3894–3899.

JP1042377